

Soft Matter

Accepted Manuscript



This is an *Accepted Manuscript*, which has been through the Royal Society of Chemistry peer review process and has been accepted for publication.

Accepted Manuscripts are published online shortly after acceptance, before technical editing, formatting and proof reading. Using this free service, authors can make their results available to the community, in citable form, before we publish the edited article. We will replace this *Accepted Manuscript* with the edited and formatted *Advance Article* as soon as it is available.

You can find more information about *Accepted Manuscripts* in the [Information for Authors](#).

Please note that technical editing may introduce minor changes to the text and/or graphics, which may alter content. The journal's standard [Terms & Conditions](#) and the [Ethical guidelines](#) still apply. In no event shall the Royal Society of Chemistry be held responsible for any errors or omissions in this *Accepted Manuscript* or any consequences arising from the use of any information it contains.



Journal Name

ARTICLE

Multiple Shape Memory Polymers Based on Laminates Formed from Thiol-Click Chemistry Based Polymerizations

M. Podgórski,^{a,b} C. Wang^a and C. N. Bowman^{a*}Received 00th January 20xx,
Accepted 00th January 20xx

DOI: 10.1039/x0xx00000x

www.rsc.org/

This investigation details the formation of polymer network trilayer laminates formed by thiol-X click chemistries, and their subsequent implementation and evaluation for quadruple shape memory behavior. Thiol-Michael addition and thiol-isocyanate-based crosslinking reactions were employed to fabricate each of the laminate's layers with independent control of the chemistry and properties of each layer and outstanding interlayer adhesion and stability. The characteristic features of step-growth thiol-X reactions, such as excellent network uniformity and narrow thermal transitions as well as their stoichiometric nature, enabled fabrication of trilayer laminates with three distinctly different glass transition temperatures grouped within a narrow range of 100 °C. Through variations in the layer thicknesses, a step-wise modulus drop as a function of temperature was achieved. This behavior allowed multi-step programming and the demonstration and quantification of quadruple shape memory performance. As is critical for this performance, the interface connecting the layers was evaluated in stoichiometric as well as off-stoichiometric systems. It was shown that the laminated structures exhibit strong interfacial binding and hardly suffer any delamination during cyclic material testing and deformation.

Introduction

Multiple shape memory polymers (MSMPs), unlike traditional dual-shape memory materials, are an advanced class of smart materials that possess at least two metastable shapes from which they can transform consecutively, upon application of the necessary stimulus, to a permanent configuration^{1–10}. The simplest example would be a material with two temporary shapes (A and B) that can recover from a distinct shape A through an intermediate configuration B, and into a final, permanent shape C. The shape memory effect in MSMPs is achieved by a multi-step programming, during which process a sample is deformed repeatedly and fixed into temporary shapes. For example, to fix two temporary shapes A and B, a two-step programming is used for a polymer structure that must allow the formation of two distinct domains comprising independent covalent or physical crosslinks^{11,12}.

Such behavior is typical for triple shape memory polymers (TSMPs). This concept was for the first time explored by Bellin et al. who prepared a TSMP by combining two crystalline switching

phases of poly(ϵ -caprolactone) (PCL) and PEG¹¹. In a similar approach, Peng and co-workers demonstrated a TSM effect utilizing a polymer network characterized with two different transition temperatures originating from a semi-crystalline phase of PEG2000 (melting temperature) and an amorphous phase of PMMA (glass transition temperature)¹³.

Following from these initial reports, significant progress has been made in the technology and chemistry of MSMPs. Utilizing various chemical and materials approaches, others have combined amorphous vs. crystalline switching phases in several polymer systems^{14–18}. Luo et al. developed a composite TSM by incorporating low-melting PCL fibers into an epoxy matrix with an appropriate glass transition temperature¹⁹. The changes in chemical composition of the fibers and the matrix allowed for control over the desired range of transitions required for several applications. Voit and coworkers designed a supramolecular vs. covalent TSMP by polymerizing UPy-functionalized (meth)acrylate monomers with n-alkyl-containing monoacrylates and acrylate crosslinkers²⁰. The glass transition temperature of the acrylate network and dissociation of self-complimentary hydrogen bonding between UPy units allowed for control of the transitions and thermomechanics of the thus made TSMPs. Polymer bilayers were shown to have a distinct TSM effect in laminated epoxy layers with two distinct glass transition temperatures²¹. Adjustments in the moduli ratios between the layers, interfacial adhesion, and T_g difference were pointed out as the key criteria in the design of a well-performing TSM material. Also, polymer blends of either semicrystalline polymers such as

^a Department of Chemical and Biological Engineering, University of Colorado, Boulder, CO, USA

^b Department of Polymer Chemistry, Faculty of Chemistry, MCS University, Lublin, Poland

E-mail: christopher.bowman@colorado.edu

Electronic Supplementary Information (ESI) available: See

DOI: 10.1039/x0xx00000x

poly(cyclooctene)/polyethylene or amorphous polymers such as polyurethane/polytetramethylene were shown to have TSM properties^{22,23}.

All of these examples describe the simplest case of MSMPs, i.e. TSMPs with triple-shape actuation capabilities. However, it was not until 2010 that Xie reported quadruple shape memory properties of thermoplastic polytetrafluoroethylene containing perfluoroether sulphonic acid side chains². His concept was based on one broad transition (T_g) considered as a spectrum of an infinite number of phase transitions. Multi-shape programming was achieved within this broad transition, with each shape recovery corresponding to infinitely sharp transition continuously distributed across the materials' T_g range. In the follow-up work the same authors described a creative strategy for using a poly(styrene-co-methyl acrylate) gradient copolymer designed in such a way as to form a V-shaped gradient sequence⁵. Its chain sequence and the resulting microphase separation allowed a very broad T_g range and even quintuple shape programming. A potential drawback of such an approach was deteriorating shape fixity (falling below 60%) with the increasing number of transitions and the temporal instability of each transitional state because of slow relaxation that continuously occurs within the broad transition range.

Recently, we showed a TSMP incorporating two distinct thiol-Michael polymer network composites with varied glass transition temperatures²⁴. The selective reaction between thiol and ene monomers has led us toward the synthesis of near-IPN type of material consisting of two thiol-Michael network domains within one sample and obtained in a one pot procedure. Specifically, divinyl sulfone (DVS) was reacted with tetramercaptoacetate thiol (PETMA) followed by subsequent reaction of a triacrylate monomer with tetramercaptopropionate thiol (TMPTMP). These two polymers have well separated and very narrow glass transitions (55 and 10°C, respectively), as is common for thiol-based step-growth materials. Their features enabled a TSM effect, which additionally possessed impressive intermediate shape stability.

Continuing our efforts, we decided to explore further the benefits of thiol-X reactions in shape memory materials preparation. As thiol-X network materials generally possess uniform structures with very narrow transitions, theoretically it should be possible to combine three separate networks with varied and rapid transitions, within a relatively narrow temperature range while still achieving excellent temporal and thermal stability associated with each of the narrow thermal transitions. The key requirement is that the transitions should not overlap and be well separated. Another prerequisite would be to have the transitions within some reasonable working temperatures, not too low and not too high. Having that in mind, it would be difficult to attain all these features using thiol-Michael chemistry only, as it usually does not allow for the formation of high T_g glasses. However, thiols are known to react rapidly with isocyanates, and the resulting thiourethane-rich networks reach glass transitions significantly higher than those formed from thiol-Michael-based polymers. Therefore, adopting a layer-by-layer methodology, similar to the one described by Xie and coworkers, we prepared laminated structures consisting of two

and three either thiol-Michael or thiol-Michael/thiol-isocyanate layers which result in triple and quadruple shape memory behavior, respectively. To facilitate interfacial bonding between the layers in a laminate, off-stoichiometric monomer mixtures were considered where the residual, unreacted thiols (or other functional groups) present in the underlying layer are available for covalent reaction with the subsequent layer. This approach assures strong, covalent coupling between the layers. Laminates were characterized by dynamic mechanical measurements, and quadruple shape memory (QSM) demonstration was recorded by video and analysis of shape and dimensional changes. Also, the interfacial bonding was evaluated in tensile experiments.

Experimental methods

Materials

Trimethylolpropane triacrylate (TMPTA), triphenylphosphine (TPP), methanesulfonic acid (MsOH), hexamethylene diisocyanate (HMDI), toluene diisocyanate (TDI) and rhodamine B were purchased from Sigma-Aldrich. Pentaerythritol tetrakis(3-mercaptopropionate) (PETMA) was purchased from TCI America. Divinyl sulfone (DVS) was purchased from Oakwood Chemicals. Trimethylolpropane tris(3-mercaptopropionate) (TMPTMP) and pentaerythritol tetrakis(3-mercaptopropionate) (PETMP) were donated from Bruno Back. All chemicals were used as received unless otherwise noted.

Methods

Dynamic Mechanical Analysis (DMA) was performed using a TA Instruments Q800 dynamic mechanical analyzer. Laminated samples as well as single polymeric layers were prepared in 0.25 or 1 mm thick glass cells. All samples were thermally treated at 80 °C for 30 min to ensure the highest conversion attainable. Samples of the dimensions 10×4×1/0.25 mm were used in the DMA tests. The temperature was ramped at 3 °C/min with a frequency of 1 Hz. The glass transition temperature(s) (T_g) were assigned as the temperature(s) at the peak of the $\tan \delta$ curve.

Shape Memory Measurements. Single film shape memory tests were conducted on a TA Instruments Q800 dynamic mechanical analyzer. Experiments were run in controlled force mode. As the limited force in the DMA instrument prevented the tests on laminated films, experiments were conducted only on neat single layers. The runs were done in duplicate. Shape fixity (R_f) and shape recovery (R_r) values were calculated from the equations:

$$R_f = \varepsilon / \varepsilon_{\max} \times 100 (\%)$$

$$R_r = (\varepsilon_{\max} - \varepsilon_{\text{final}}) / \varepsilon_{\max} \times 100 (\%)$$

In the equations ε , ε_{\max} , and $\varepsilon_{\text{final}}$ represent the strain after shape-fixing, the maximum strain attained, and the final strain after each shape memory cycle, respectively.

QSM tests were performed on the laminate stripes coiled around cylindrical mandrels of different diameters. Shape fixity and shape recovery values were obtained by comparing the differences in diameters for the achieved shapes after each step of programming ($R_f = d_{\text{prog}}/d_{\text{fix}} \times 100\%$) and subsequent recovery ($R_r = d_{\text{prog}}/d_{\text{rec}} \times 100\%$) to the diameters of the respective cylinders used. In these equations d_{prog} is the diameter of cylinder used for programming, d_{fix} is the diameter within the circular sample after releasing of the strain, and d_{rec} is the diameter of the subsequently recovered circular shape.

Fabrication of Laminates. As detailed previously, TPP/MsOH (1/0.2 wt %) was used as a time-delayed initiator system for the thiol–Michael addition, and TPP/MsOH/DVS (1/0.2/3 wt %) was used for the thiol-isocyanate reaction, respectively^{25,26}. In the case of the thiol–Michael reaction, TPP and MsOH were dissolved in the thiol, and then the thiol was mixed with the vinyl monomer until a homogenous mixture was obtained. In the case of the thiol-isocyanate reaction, TPP and MsOH were added to the thiol, DVS was added to the isocyanate, and then both mixtures were combined and homogenized.

The laminates were prepared in the layer-by-layer technique in glass cells with varied thickness of the separating spacers. The spacers of the sizes 0.05, 0.1, 0.25, and 1 mm were used. Basically, a monomer mixture was poured into glass mold with given thickness depending on the type of the laminated structure. After the polymerization, one glass slide was removed, new spacers were inserted, and a fresh monomer mixture was poured on top of the previously polymerized film. To achieve the desired thickness, another glass slide was put on top of the reacting mixture and pressed gently against the spacers. To fabricate a three-layered laminate this last step was repeated one more time. After 15 min per layer reaction at ambient temperature, the laminate sample was postcured at 80 °C for an additional 30 min to ensure quantitative conversions.

The layers in the laminates consisted of mixtures of TMPTMP/TMPTA, PETMA/DVS, PETMP/HMDI or PETMP/HMDI/TDI. Either 10wt % excess of the thiol or vinyl/isocyanate monomer was also considered to improve the interfacial bonding.

To validate the uniformity of the thus prepared laminates, rhodamine B dye was added in the upper and bottom layers during the preparation of an exemplary three-layered laminate. Subsequently, microscopic images were collected capturing the interface within the tested laminate. As is depicted in Fig. 1, a uniform laminated structure with a very well defined interface and precise layer thickness was revealed.

Tensile testing. Tensile experiments were conducted on dual-type rectangular samples comprised of two types of polymeric materials bonded at the cross-section. The sample sizes were 10/4/1 mm with the bonding cross-section located in the middle of the sample. Similar to the laminate preparation technique, the dual-type samples were prepared by polymerizing a given

mixture of monomers being placed in contact with the already polymerized film. The interface texture was that of the 1 mm thick glass slide used as the spacer during preparation of the initial film. PETMA/DVS and PETMP/HMDI stoichiometric and off-stoichiometric mixtures were selected for the interfacial bonding testing. In the off-stoichiometric experiments, 10 wt % excess of HMDI and PETMA or PETMP and DVS was used. All samples were thermally annealed at 80 °C for 30 min. The tensile tests were performed at ambient conditions with the crosshead speed of 2 mm/min.

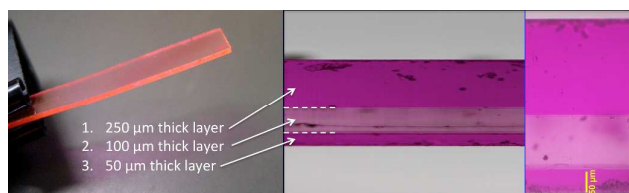


Fig. 1. Microscopic images of a side view of an exemplary 0.4 mm thick three-layered laminate in three different enlargements. The laminate specimen having two layers dyed with rhodamine B is depicted on the left side of the figure. The close-up images show three distinct layers with well defined thicknesses.

Results and discussion

Bilayer and trilayer laminates

As a proof of concept, two bilayer laminates were prepared and tested for their shape memory behavior. Analogous to the networks employed in our recent TSM composite example²⁴, the same monomers were utilized here to fabricate the layers of a bilayer film.

Specifically, an off-stoichiometric mixture of PETMA/DVS (10 wt% excess thiol) was polymerized on top of a TMPTMP/TMPTA (10 wt % excess acrylate) film. Two bilayers were formed from different relative ratios of the layer thicknesses, i.e. the TMPTMP/TMPTA layer had a thickness of 250 μm, whereas the PETMA/DVS layer thickness varied, and was either 100 or 50 μm. The DMA profiles for these bilayer samples are presented in Fig. 2. Both polymeric bilayers have three discernible plateaus in their storage moduli vs. temperature behavior, which is a characteristic feature of TSM materials based on two transitions. The maxima on the tan delta curves reflect the glass transitions of the layers, and match closely those reported previously which were 10 and 55 °C, respectively. The slightly lower T_g values obtained here are due to the component off-stoichiometry in the layers resulting in somewhat reduced crosslinking densities. It is evident that the position of the mid-plateau depends on the ratio between the layers in the samples. Further, the lowest T_g layer, i.e. TMPTMP/TMPTA can be programmed at sub-ambient temperature only, which may not be practical for MSM implementations. Nevertheless, it was implemented here to facilitate the shape memory demonstration within temperatures that do not exceed 100 °C.

By changing the relative thicknesses of the two compositions, the balance in the stress between the layers would be affected during TSM programming, and the TSM effect could be tuned to be either stronger or weaker. For best performance both differences in the modulus values on either side of the mid-modulus should be possibly the largest. Therefore, the bilayer analyzed in Fig 2b represents a better TSM laminate.

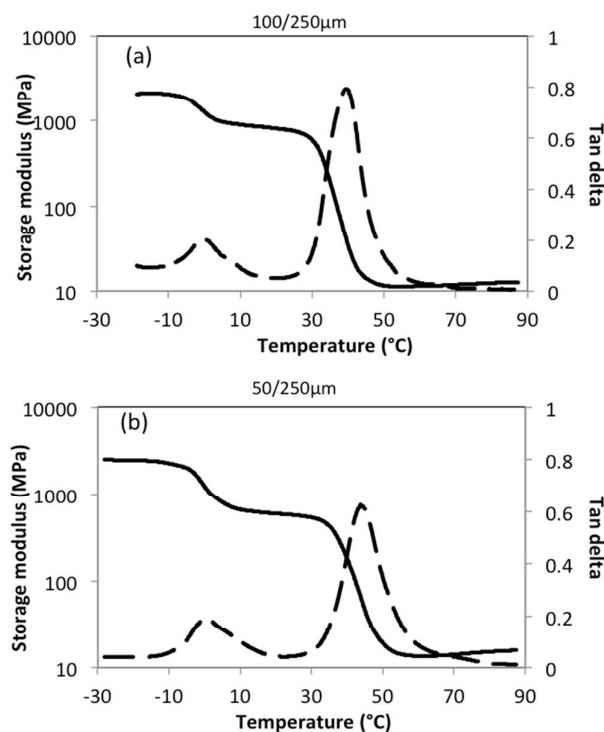


Fig. 2. Dynamic mechanical analysis of the bilayer polymers consisting of off-stoichiometric mixtures of TMPTMP/TMPTA (10 wt % acrylate excess) and PETMA/DVS (10 wt % thiol excess): the TMPTMP/TMPTA layer was 250 μm thick in both bilayers. The thickness of the PETMA/DVS layer was either 100 (a) or 50 μm (b). It is evident from the figure that decreasing the second layer thickness lowers the mid-modulus plateau. As the difference between the mid-modulus and glassy modulus is increased, the TSM behavior is expected to improve.

However, we did not run a TSM test on any of these two bilayer laminates, as it is more interesting to increase the degree of complexity and introduce a third layer in an attempt to demonstrate quadruple shape memory behavior. Thiol-X chemistry is ideal for this purpose as it produces uniform, narrow transition polymer networks²⁷. To introduce a third material, it is more practical for it to be in the higher temperature range, i.e. above the glass transition of PETMA/DVS. Therefore, we chose a thiourethane network resulting from the reaction of the tetrathiol PETMP and the diisocyanate HMDI. Both these reactants are liquids, and their mixture retains sufficient stability

to provide time to fabricate the laminate. Based on the same principles of making bilayers, the relative layer thickness in the trilayer laminate should decrease with increasing glass transition temperature of the layer. Originally, a trilayer laminate was prepared containing 250 μm thick TMPTMP/TMPTA film, 100 μm thick PETMA/DVS film, and 50 μm thick PETMP/HMDI film. The softest thiol acrylate layer was chosen to be the middle part of the laminate with the simultaneous goal of improving the laminate' toughness. All thiol-X layers were made in slight (10 wt%) off-stoichiometric ratios with the middle layer having acrylate excess, and the side layers both having thiol excess, respectively. The DMA profile of a trilayer made in such a manner is depicted in Fig. 3a. As expected, the DMA plots had all the features of a QSM material such as three transitions and four distinct plateaus on the modulus, but the highest two transitions were still too close to each other. Improving on that, TDI was added in the highest T_g layer by replacing 10 wt % of the original HMDI content. Increasing the thiourethane network stiffness enabled a material with yet higher T_g as is shown in Fig. 3b. To fabricate a QSM material with all its T_g 's above ambient, it would likely be necessary to have at least one laminate layer with a transition temperature close to or higher than 100 $^{\circ}\text{C}$. It is possible to achieve that behavior for example by using higher concentrations of structurally stiffer aromatic diisocyanates such as the TDI example previously discussed. Changing the relative concentrations of the two isocyanates, or acrylates for that matter, is a very convenient method to tune the materials' T_g . A pure PETMP/TDI network reaches T_g values as high as 145 $^{\circ}\text{C}$, and still retains impressive uniformity as indicated by the tan delta half-width value of 19 $^{\circ}\text{C}$ (Fig. S1).

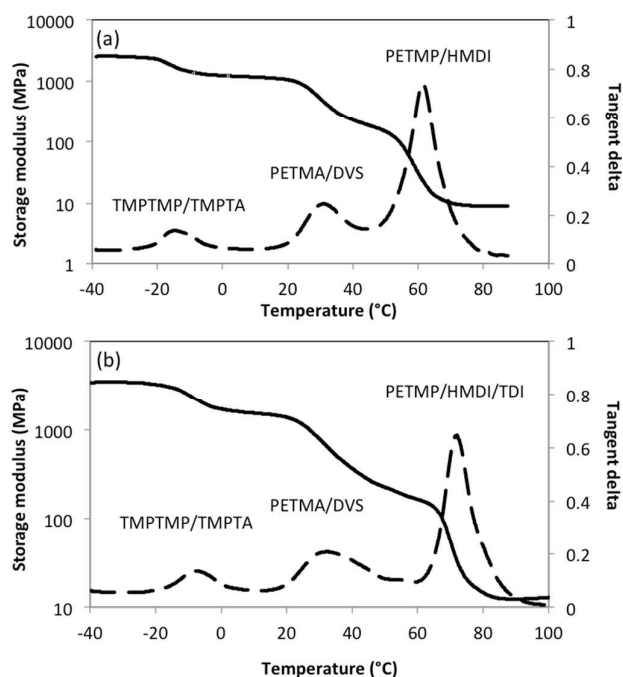


Fig. 3. Dynamic mechanical analysis of trilayer polymer laminates consisting of off-stoichiometric layers of PETMA/DVS (10 wt % thiol excess), TMPTMP/TMPTA (10 wt % acrylate excess) and PETMP/HMDI or PETMP/HMDI/TDI (10 wt % thiol excess): the ratio between the layer thicknesses was 100/250/50 μm for the layers of PETMA/DVS, TMPTMP/TMPTA, and PETMP/HMDI (a) or PETMP/HMDI/TDI (b). The inclusion of 10 wt % of TDI instead of HMDI (b) improved the T_g differences between the layers in the laminate by increasing the T_g of the thiol-isocyanate layer.

Single-film shape memory tests

As the MSM effect is dependent on the shape memory performance of each independent layer, the thiol-X single films, here made in stoichiometric ratios, were initially assessed for their shape memory properties. Shape fixity (R_f) and shape recovery (R_r) values were measured in tensile tests in the DMA. Duplicate dual-shape memory cycles with the relevant R_f and R_r values are included in Fig 4.

QSM tests

To test the SM capabilities of network materials, others have relied on a three point bending configuration which is not as limited by accessible forces or extent of sample deformation as in the case of the tensile mode^{21,28,29}. Even though the thiol-based networks are characterized by limited extent of maximal deformation, especially when subjected to external stresses above their T_g 's, here the thiol-X networks were deformed without failure up to 12 % strain in tensile experiments. Within this strain/stress range all three types of samples showed very good SM properties as denoted by the R_f and R_r values estimated in the range of 100-96 % and 91-87 %, respectively. Interestingly, post-test sample examination revealed 100 % shape recovery (R_r) in all samples disclosing the methods' limitations. Therefore, it can be concluded that the SM properties of the thiol-X polymers should be sufficient to reproduce a QSM behavior when combined in a trilayer. For the QSM demonstration a trilayer laminate made of a 250 μm thick TMPTMP/TMPTA film, a 100 μm thick PETMA/DVS film, and a 50 μm thick PETMP/HMDI/TDI film was selected with characteristic features as detailed in Fig. 3b. A laminate strip of the dimensions 100/8/0.4 mm was subjected to a three-step programming at the temperatures of 75, 45, and 0 $^\circ\text{C}$, respectively. In Scheme 1 subsequent shape recovery steps are displayed.

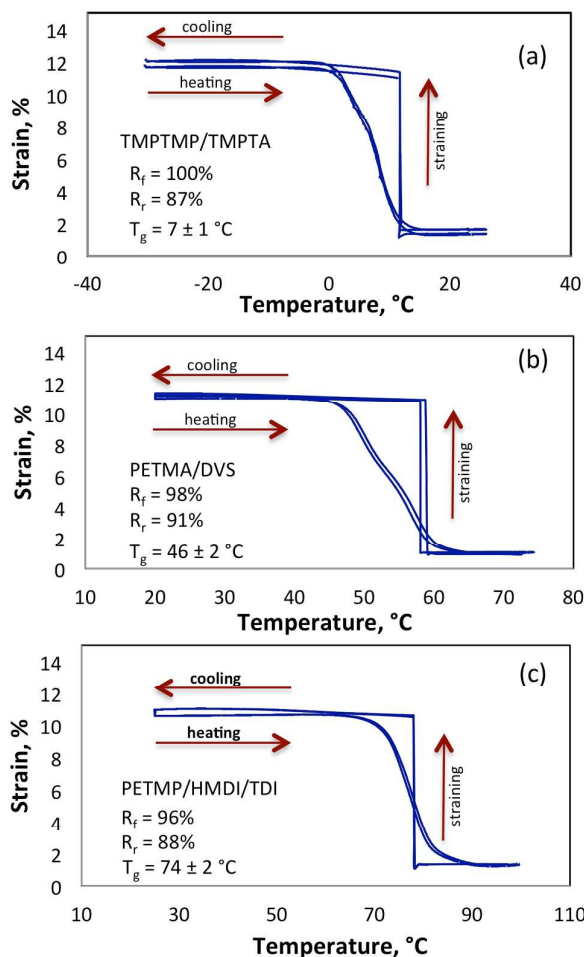
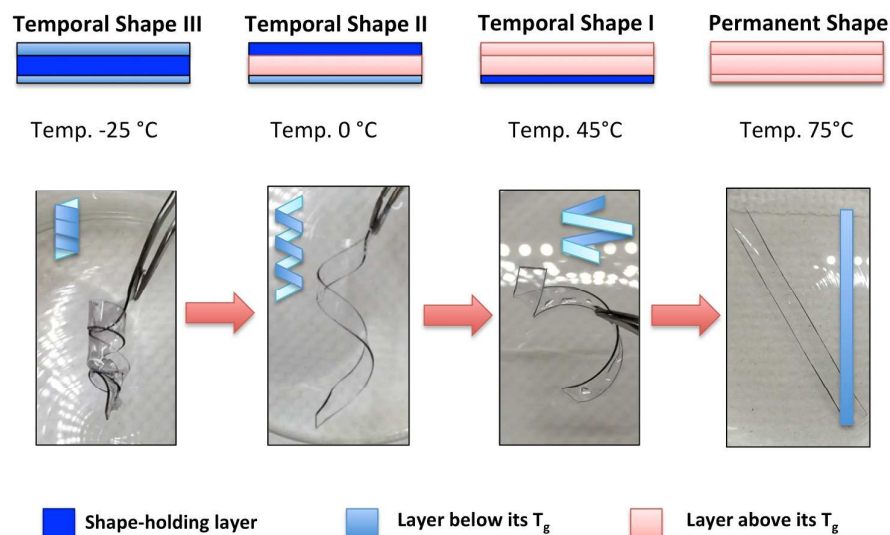


Fig. 4. Dual-shape memory cycles taken in duplicate around each individual T_g for: TMPTMP/TMPTA (a); PETMA/DVS (b); PETMP/HMDI/TDI (c). 10/4/1 mm samples were analyzed. All samples prepared in a 1:1 stoichiometric ratio of thiols to acrylates, isocyanates or vinyl sulfones. R_f and R_r values as well as the layers' T_g 's are also included in the figure.



Journal Name

ARTICLE



Scheme 1. Schematic of quadruple shape recovery cycle in a trilayer laminate. At a temperature of -25 °C the thickest 250 μm middle layer holds the compressed spring shape – i.e., temporal shape III. Then, the spring unfolds into temporal shape II at 0 °C, i.e. the shape maintained by the 100 μm thick layer. At 45 °C temporal shape I (a reversed spring) is recovered as programmed within the last, thinnest layer. At 75 °C the recovery track is completed when the permanent shape is recovered.

Table 1. Summary of quadruple shape memory (QSM) properties and their dependence on the direction of the laminates' deformation. The shape fixity (R_f) was based on the relation $R_f = d_{\text{prog}}/d_{\text{fix}} \times 100 \%$, whereas the shape recovery was obtained from $R_r = d_{\text{prog}}/d_{\text{rec}} \times 100 \%$.

Test #	Bending direction	R_f (A \rightarrow B) (%)	R_f (B \rightarrow C) (%)	R_f (C \rightarrow D) (%)	R_r (D \rightarrow C) (%)	R_r (C \rightarrow B) (%)	R_r (B \rightarrow A) (%)
1	Toward layer A (\rightarrow ABC)	84 (3)	93 (3)	91 (2)	97 (3)	88 (2)	100 (-)
2	Away from layer A (\rightarrow CBA)	73 (3)	82 (4)	99 (1)	94 (3)	71 (3)	100 (-)

More importantly, supporting information video SV1 shows a recorded QSM demonstration, which is in accordance with the graphic and photos in Scheme 1. The three recovery steps include: unfolding of a compressed spring at 0 °C, transformation into a reversed spring at 45 °C, and permanent shape recovery at 75 °C. This result is one of a very few examples showing a QSM transformation in a single sequence. It also nicely demonstrates the versatility and potential of thiol-X click chemistry for making ideal polymer networks.

To quantify the shape fixity and recovery parameters during quadruple programming and recovery cycles, the QSM laminate sample was coiled repeatedly at decreasing temperatures around three well-defined cylinders of decreasing diameters (d). In principle, permanent shape A was first deformed around the largest cylinder at the highest temperature of 80 °C ($d = 27 \text{ mm}$) and the first temporal shape B was fixed at 45 °C. Then, temporal shape B was further deformed on a medium-sized cylinder with $d = 15 \text{ mm}$, thus resulting in shape C fixed at 0-5 °C. Finally, the third temporal shape D was achieved by coiling the sample more

around a cylinder of 10 mm in diameter and fixing the shape below $-20\text{ }^{\circ}\text{C}$. The pictures describing the shape recovery cycles can be found in supporting information Fig. S2. Also, the degree of dependence of fixing/recovery on the direction of bending was determined. The degree of directionality of bending in a laminate consisting of layers ABC was assessed by deforming the laminate first toward layer A, and then away from layer A, i.e. towards layer C (Table 1). The tabulated data indicates strong dependence of fixing on the direction of laminate deformation. It is most obvious in the first step of high temperature programming where the shape-holding outer layer A is subjected to larger or lesser stresses depending on the direction of bending as denoted by the R_f ($A \rightarrow B$) and R_r ($C \rightarrow B$) values, respectively. During the initial shape fixing at the highest temperatures, the layers B and C are in their rubbery state, and therefore are expected to counterbalance the programmed shape proportionally to the degree of their deformation (straining).

When the laminate is deformed toward layer A, layer A is under higher strain than the other layers as they are further away from the cylinder surface, therefore overlapped over an effectively larger radius. In the opposite case, the layer A being the outermost layer from the surface of the cylinder is subjected to less strain than layers B and C. Consequently, layer A holds its shape better when it is strained more, whereas the other layers are strained less at the same time, than in the opposite case when layer A is subject to less strain than the other layers. This trend is also apparent in the second step of programming, but seems to be insignificant in the last step where the middle and the thickest layer holds the third programmed shape. Concluding, there are multiple factors such as the thickness, the order of the layers and their respective moduli at the shape fixing temperatures as well as the direction of deformation to be considered to achieve the optimal MSM effect.

Laminate interfacial adhesion

One important requirement of any laminated structure is good interfacial adhesion³⁰. This necessity holds true, especially for shape memory laminates as they are subjected to large deformations and interfacial stresses during programming/recovery cycles. Any delamination that occurs would compromise the laminate's performance. Because of the self-limiting character of step-growth thiol-X polymerizations, these reactions can be carried out off-stoichiometrically, which leaves residual functionality accessible on the surface and throughout the material for further modification reactions. Polymerizing an off-stoichiometric thiol-X mixture on top of an off-stoichiometric thiol-X film promotes covalent linking between the layers. The interface was evaluated between two different types of thiol-X substrates in systems with balanced stoichiometry as well as in off-stoichiometric mixtures. The characteristic stress vs. strain profiles for two-component samples that were welded at the cross-section are presented in Fig. 5.

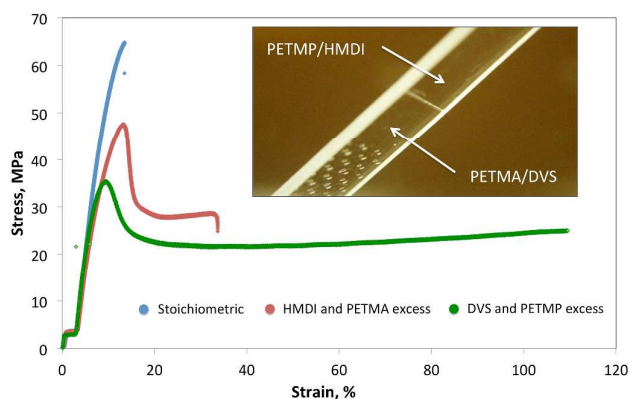


Fig. 5. Stress-strain plots of bimodal thiol-X overlapping adhesion samples. The compositions that were combined into two-component specimens were mixtures of PETMA/DVS and PETMP/HMDI. The inset in the figure displays the bonding cross-section of an exemplary sample. Three types of thiol-X two-component samples were tested: PETMP/HMDI-PETMA/DVS (stoichiometric), PETMP/HMDI-PETMA/DVS (off-stoichiometric – 10 wt % isocyanate and thiol excess in each layer) and PETMP/HMDI-PETMA/DVS (off-stoichiometric – 10 wt % vinyl and thiol excess in each layer). Only the stoichiometric samples yielded at the cross-section after reaching an impressive stress exceeding 60 MPa. The off-stoichiometric samples yielded through substrate failure.

To pull apart the thiol-X materials bound together in the cross-section area requires a significant amount of force. The cross-section fails only in case of the stoichiometric mixtures. In the two off-stoichiometric systems, both yielded in areas beyond the interfacial overlapping region, through substrate failure. This suggests, that the binding interface in off-stoichiometric films is stronger than the films themselves, indicating that a satisfactory level of interfacial adhesion is achieved. This outcome is confirmed in the three-step programming/recovery experiments of the laminated sample used for QSM tests, as we did not observe any delamination even after extensive and repeated laminate deformation.

Conclusions

The versatile nature of thiol-X reactions was demonstrated to be useful for the formation of multiple shape memory behavior of laminates. The time-delayed reaction onset in the otherwise rapidly reacting mixtures enabled facile layer-by-layer laminate fabrication. Laminates having three different thiol-Michael or thiol-isocyanate polymeric layers were formed and evaluated for their shape memory properties and layer-to-layer adhesion. It was demonstrated that the shape memory effect relying on the T_g separation in the layers could be tuned by the changes in chemistry involved and the off-stoichiometric imbalance. Further, the thickness of the layers was shown to be well maintained, and controlled, facilitating shape-to-shape

Journal Name

ARTICLE

transformations and programming. On the other hand, the interfacial adhesion between the layers was shown to have sufficient strength to withstand the deformations imposed on the laminate without failure. As a whole, the laminated composites made in trilayers exhibited good quadruple shape memory properties as quantified by the values of R_f and R_r from QSM tests.

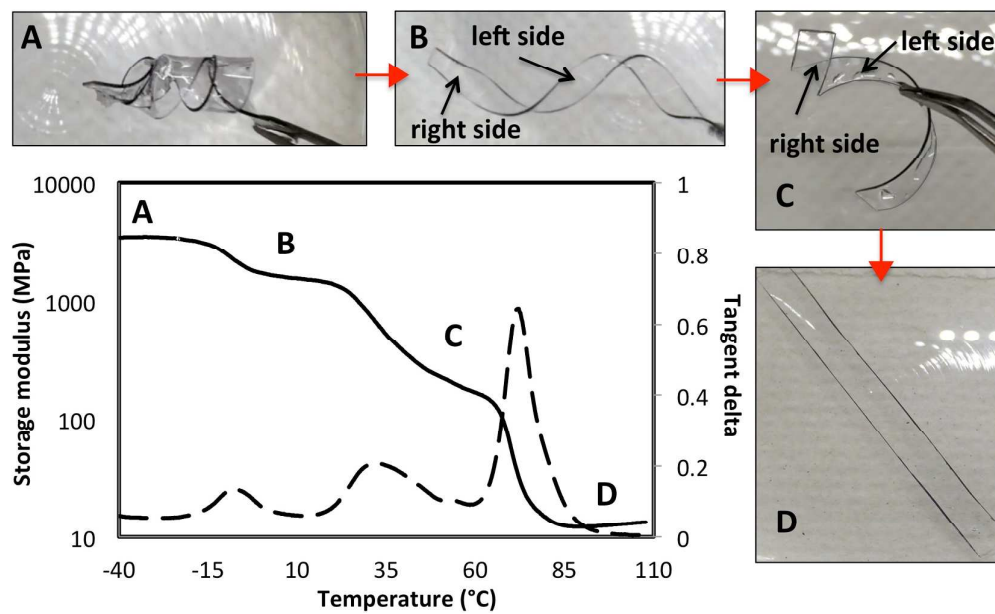
Acknowledgements

We would like to acknowledge the following sources of funding: the National Institutes of Health (1U01DE023777-01), and the National Science Foundation (CHE-1214109) and (DMR-1310528).

Notes and references

- 1 Q. Zhao, H. J. Qi and T. Xie, *Prog. Polym. Sci.*, 2015, doi:10.1016/j.progpolymsci.2015.04.001
- 2 T. Xie, *Nature*, 2010, **464**, 267–270.
- 3 M. Wei, M. Zhan, D. Yu, H. Xie, M. He, K. Yang and Y. Wang, *ACS Appl. Mater. Interfaces*, 2015, **7**, 2585–2596.
- 4 R. Xiao, J. Guo and T. D. Nguyen, *RSC Adv.*, 2015, **5**, 416–423.
- 5 Y. Luo, Y. Guo, X. Gao, B. G. Li and T. Xie, *Adv. Mater.*, 2013, **25**, 743–748.
- 6 J. Li, T. Liu, S. Xia, Y. Pan, Z. Zheng, X. Ding and Y. Peng, *J. Mater. Chem.*, 2011, **21**, 12213.
- 7 T. Xie, *Polymer (Guildf.)*, 2011, **52**, 4985–5000.
- 8 J. Hu, Y. Zhu, H. Huang and J. Lu, *Prog. Polym. Sci.*, 2012, **37**, 1720–1763.
- 9 W. H. De Jeu, J. J. H. Kausch, S. K. K. Lee, T. E. L. I. Manners, M. M. O. Nuyken and B. V. G. W. U. Wiesner, *Advances in Polymer Science*, 2006.
- 10 G. J. Berg, M. K. McBride, C. Wang and C. N. Bowman, *Polymer (Guildf.)*, 2014, **55**, 1–24.
- 11 I. Bellin, S. Kelch, R. Langer and a Lendlein, *Proc. Natl. Acad. Sci. U. S. A.*, 2006, **103**, 18043–18047.
- 12 M. Bothe, K. Y. Mya, E. M. Jie Lin, C. C. Yeo, X. Lu, C. He and T. Pertsch, *Soft Matter*, 2012, **8**, 965.
- 13 P. Ping, W. Wang, X. Chen and X. Jing, *Biomacromolecules*, 2005, **6**, 587–592.
- 14 F. Chen, M. Huang and X. Dong, *ACS Appl. Mater. Interfaces*, 2014, **6**, 20051–20059.
- 15 S. Chena, J. Hua, C. W. Yuena, L. Chana and H. Zhuoa, *Polym. Adv. Technol.*, 2010, **21**, 377–380.
- 16 H. B. Nejad, R. M. Baker and P. T. Mather, *Soft Matter*, 2014, **10**, 8066–8074.
- 17 Y. Shao, C. Lavigueur and X. X. Zhu, *Macromolecules*, 2012, **45**, 1924–1930.
- 18 Y. Kim, H. Park and B. Kim, *High Perform. Polym.*, 2015.
- 19 X. Luo and P. T. Mather, *Adv. Funct. Mater.*, 2010, **20**, 2649–2656.
- 20 T. Ware, K. Hearon, A. Lonneckner, K. L. Wooley, D. J. Maitland and W. Voit, *Macromolecules*, 2012, **45**, 1062–1069.
- 21 T. Xie, X. Xiao and Y. T. Cheng, *Macromol. Rapid Commun.*, 2009, **30**, 1823–1827.
- 22 J. M. Cuevas, R. Rubio, L. Germán, J. M. Laza, J. L. Vilas, M. Rodriguez and L. M. León, *Soft Matter*, 2012, **8**, 4928.
- 23 S.-Y. Gu, L.-L. Liu and X.-F. Gao, *Polym. Int.*, 2015, DOI 10.1002/pi.4886
- 24 S. Chatani, C. Wang, M. Podgórski and C. N. Bowman, *Macromolecules*, 2014, **47**, 4949–4954.
- 25 S. Chatani, R. J. Sheridan, M. Podgórski, D. P. Nair and C. N. Bowman, *Chem. Mater.*, 2013, **25**, 3897–3901.
- 26 M. Podgórski, D. P. Nair, S. Chatani, G. Berg and C. N. Bowman, *ACS Appl. Mater. Interfaces*, 2014, **6**, 6111–6119.
- 27 D. P. Nair, M. Podgórski, S. Chatani, T. Gong, W. Xi, C. R. Fenoli and C. N. Bowman, *Chem. Mater.*, 2014, **26**, 724–744.
- 28 B. Yang, W. M. Huang, C. Li, C. M. Lee and L. Li, *Smart Mater. Struct.*, 2003, **13**, 191–195.
- 29 Y. Liu, K. Gall, M. L. Dunn and P. McCluskey, *Smart Mater. Struct.*, 2003, **12**, 947–954.
- 30 C. Y. Bae, J. H. Park, E. Y. Kim, Y. S. Kang and B. K. Kim, *J. Mater. Chem.*, 2011, **21**, 11288.

TOC Graphic



Polymer network trilayer laminates formed by thiol-Michael and thiol-isocyanate click chemistries, and their subsequent implementation and evaluation for quadruple shape memory (QSM) behavior is presented.